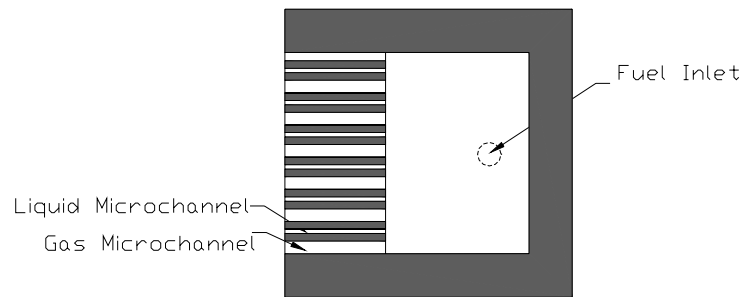


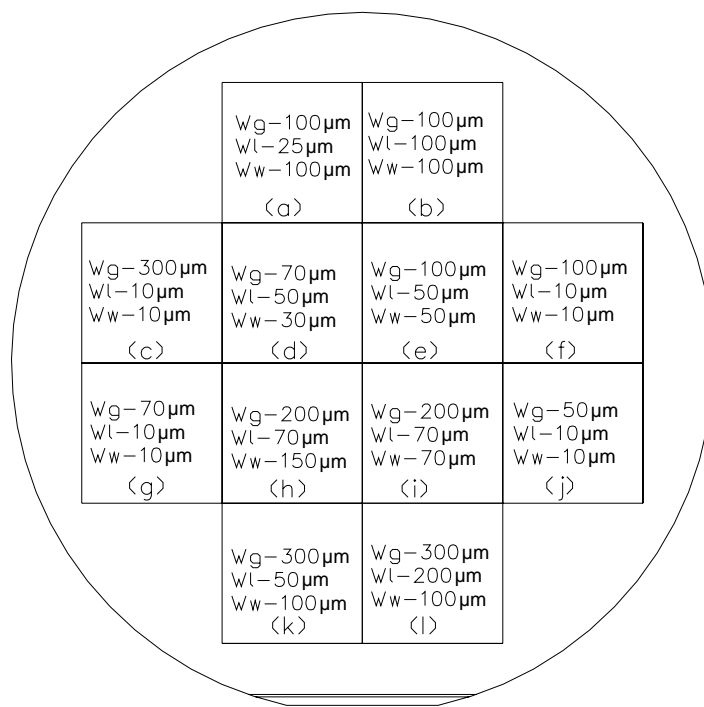
4. Experimental Results and Discussion

4.1 Preliminary Experimental Method

Before fabricating the bubble separator as described in Fig. 3.1, preliminary experiment samples with width-different microchannel structures were fabricated and tested. The preliminary experiment was designed to determine the optimal microchannel widths so that the CO₂ bubbles can be separated from the two-phase flow effectively. Wet etching was used to generate liquid microchannels, gas microchannels, and dividing walls with different sizes, as in Fig. 4.1. Different combinations of wide and narrow microchannels with dividing walls having different sizes were fabricated. As shown in Fig. 4.1, the width of the wider microchannels (W_g) ranged from 50 to 300 μm , the width of the narrower microchannels ranged from 10 to 200 μm , and the width of the dividing wall ranged from 10 to 150 μm . The smallest wall width of 10 μm was selected to test if good microchannel structures could be obtained in our fabrication process.



(a)



(b)

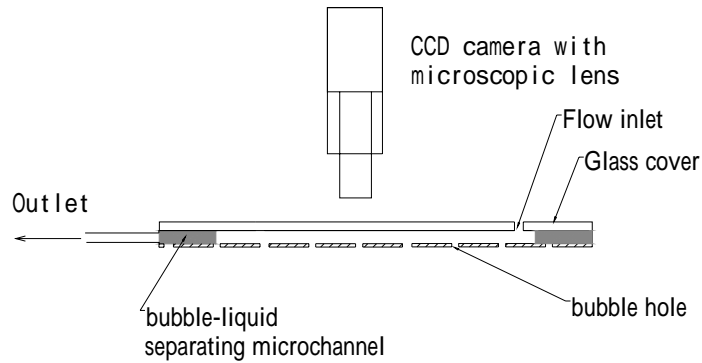
Figure 4.1 (a) preliminary experiment sample structure including microchannels with different widths

(b) parameters: W_g -- the width of gas microchannel
 W_l -- the width of liquid microchannel
 W_w —the thickness of wall

In this experiment, DI water was injected with a syringe into the open-top sample. The liquid behavior was then observed when it touched the microchannel entrances. It was found that microchannels with width smaller than 25 μm could not only suck the liquid by capillary force but also prevent bubbles flow in them by threshold pressure; microchannels with width greater than 100 μm could hardly suck the liquid. Therefore, the widths of 25 μm and 100 μm are respectively selected for the liquid and gas microchannels in the bubble separator to be designed and fabricated.

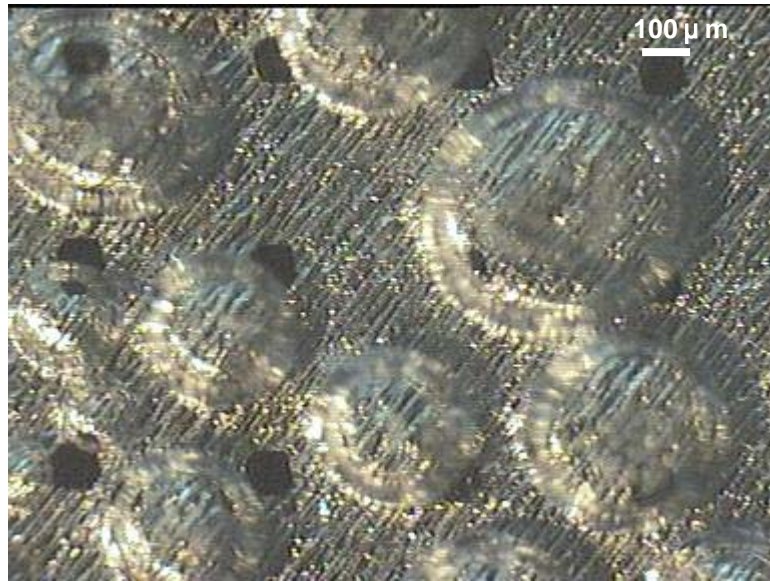
4.2 Experimental Results for Bubble Separator

After the preliminary experiment, the separator as in Fig. 3.1 with optimal parameters was subsequently fabricated following the process in Figure 3.2. To observe the performance, the separator was covered with a glass plate with a hole as fluid inlet. Multi-direction bubble removal capability was examined by setting the separator horizontally with the microholes facing downward. The process of bubble removal was recorded with a CCD camera, as shown in the Fig. 4.2. The CO_2 bubbles in the experiment were generated with gasified water which was injected into the sample chamber by a syringe, to simulate bubbles in the anode of μDMFC .

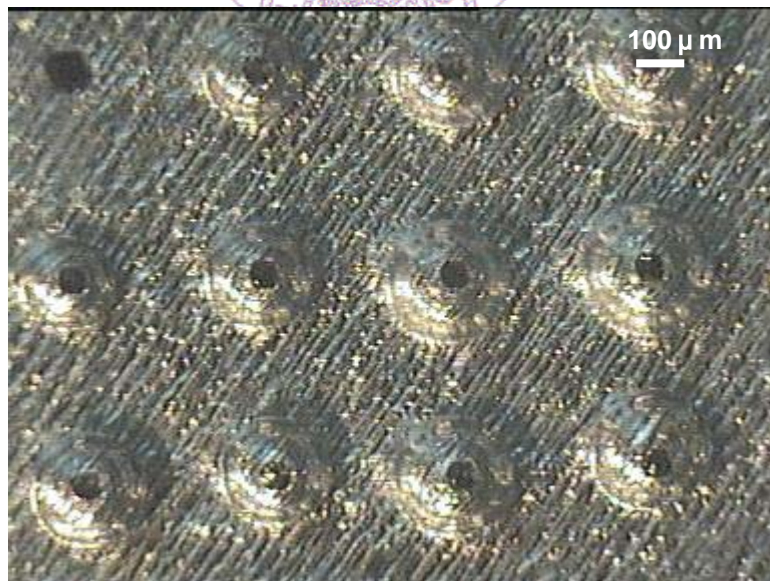


4.2 Experimental equipment setup for bubble separation

Bubble separation was first observed for the flat section with only microholes. Fig. 4.3 compares the bubble behaviors under two situations: (a) a sample having merely hydrophilic surfaces for both the flat surface of the plate and the surface in the holes and (b) a sample having hydrophilic flat surface but hydrophobic holes. In situation (b), bubbles automatically move to the hydrophobic holes due to capillary force. Most of the gas in the bubbles was ejected leaving only small bubbles around the holes, as shown in Fig. 4.3(b). The residual diameters of the bubbles range from 150 to 300 μm . The hole diameter appears smaller than the actual size because the bubble serves as a lens. It is noted that upper left hole in Fig. 4.3(b) is not attached with a bubble. It is speculated that the liquid-gas interface exists within the hole because the hydrophobic Teflon® layer didn't wet to the upper surface. The experiment confirms that CO_2 bubbles in a liquid flow can indeed be captured by hydrophobic holes on a hydrophilic surface, and partially exhausted. In comparison, the bubbles could not be captured and exhausted in situation (a), in which randomly distributed bubbles spread over the plate, as shown in Fig. 4.3(a).



(a)



(b)

Fig. 4.3 Bubbles on the bubble separator plate. (a) Bubbles randomly distributed and could not be exhausted through hydrophilic hole array. (b) bubbles captured and partially exhausted on hydrophobic hole array.

In the microchannel section of the separation, there are alternating hydrophilic liquid microchannels and gas hydrophobic microchannels with holes as shown in Fig. 4.4. It is noted that the wall ends are formed in irregular slope because the silicon crystallography of the sidewall cannot defend the KOH solution. This affects the Teflon® coating near the ends. As stated in section 3.2, the Teflon® coating in the gas microchannels was rendered by the capillary suction. The irregular slope provides weaker capillary ability and causes defect of coating at the coating wall ends. This is reflected in Fig. 4.5. In Fig. 4.5, the DI water is successfully sucked into the hydrophilic liquid microchannels but effectively prevented in the hydrophobic microchannels, except near the wall ends.

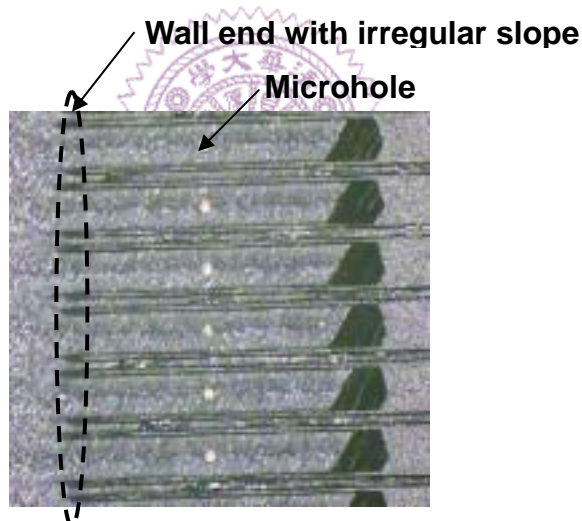


Fig. 4.4 The microchannel structure on the separator

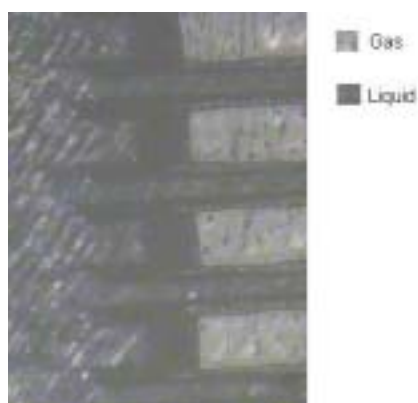


Fig. 4.5 sucking of liquid in the liquid microchannels

The bubble exhalation by the gas microchannel is shown in Figs. 4.6 and 4.7. In the experiment, gasified water is injected into the chamber. Fig 4.6 shows that a small single bubble is captured by a gas microchannel and exhausted automatically after 28 seconds. Shown in Fig. 4.7 (a)-(h) is a large bubble captured by the two gas microchannel entrances and breathed out in 30 seconds.

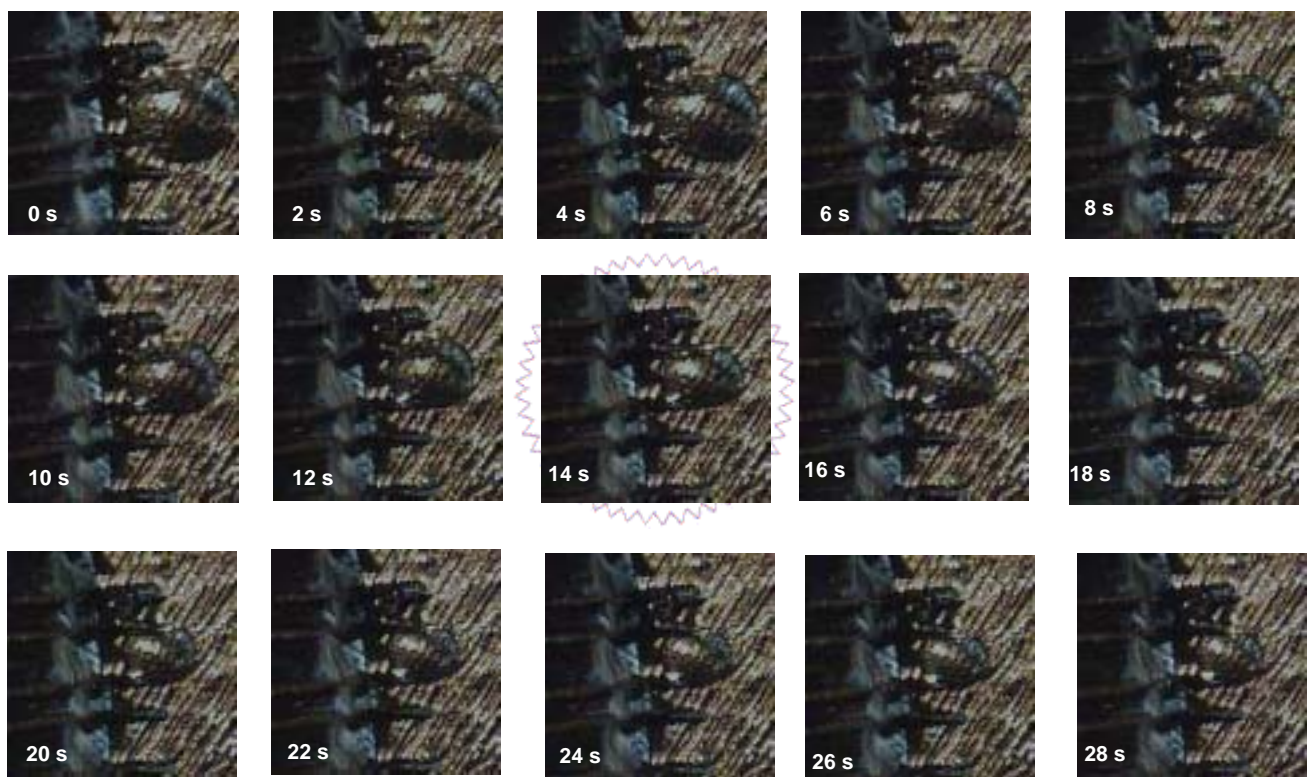


Fig. 4.6 Single CO₂ bubble separated from the liquid and breathed out in about 28 seconds.

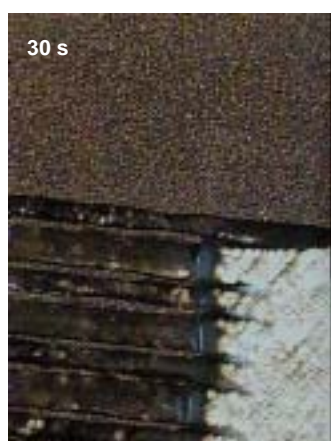
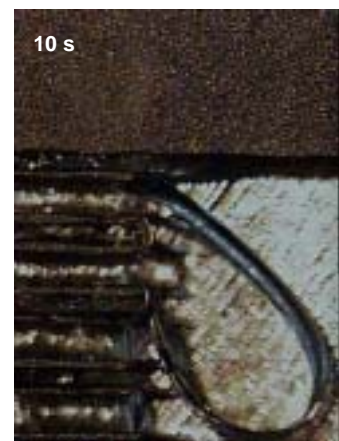
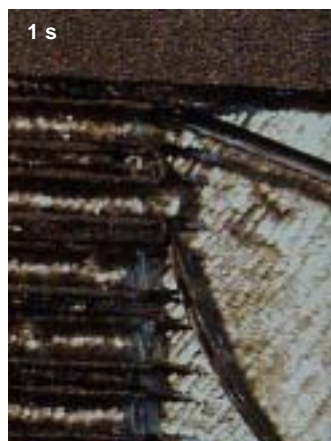


Fig. 4.7

(a) A bubble captured by the gas microchannels.

(b)~(f) The bubble exhausted from two gas microchannels

(g) The bubble breathed out completely.

4.3 Discussion

It has been shown that CO₂ bubbles generated from gasified water can be exhausted successfully through the hydrophobic holes on the hydrophilic surface and the gas hydrophobic microchannels, even when the sample is put in an anti-buoyancy direction. In addition, fuel recycling can be achieved through the narrower liquid hydrophilic microchannels. However, there are still some problems to be studied.

First, the hydrophobicity of the Teflon® which is produced by DuPont Company seems to decay after repeated tests. Heating at a higher temperature to remove the hydrophilic solvent in the Teflon® solution may improve this problem.

Secondly, the present experiments were conducted without forced fuel feeding. If there is a fuel pump to push the fuel flow steadily or oscillatorily, bubble separation is expected to be enhanced. Furthermore, According to the Young-Laplace equation, $\Delta P = -2\sigma \cos \theta \left(\frac{1}{W} + \frac{1}{H} \right)$ [18], the leakage pressure for the gas microchannel can be determined by the surface tension, the contact angle (120°), the microchannel width W (100 μm) and depth H (250 μm). With the present large width of 100 μm, the leakage pressure is only 2.55 kPa. But if the width is reduced to, say, 10 μm, the leakage pressure can be increased to about 25 kPa.

Thirdly, it should be noted that the surface tension of fuel solution with a higher methanol concentration decreases significantly. Consequently, the leakage problem becomes more serious. Using hydrophobic porous membrane with submicron effective hole diameter as the bubble separator

material has been shown to have high leakage pressure [8].

